

Defect physics and electronic properties of Cu_3PSe_4 from first principles

D. H. Foster,¹ F. L. Barras,¹ J. M. Vielma,¹ and G. Schneider^{1,*}

¹*Department of Physics, Oregon State University, Corvallis, Oregon 97331, USA*

(Dated: September 27, 2012)

The p -type semiconductor Cu_3PSe_4 has recently been established to have a direct bandgap of 1.4 eV and an optical absorption spectrum similar to GaAs [Applied Physics Letters, 99, 181903 (2011)], suggesting a possible application as a solar photovoltaic absorber. Here we calculate the thermodynamic stability, defect energies and concentrations, and several material properties of Cu_3PSe_4 using a wholly GGA+ U method (the generalized gradient approximation of density functional theory with a Hubbard U term included for the Cu- d orbitals). We find that two low energy acceptor-type defects, the copper vacancy V_{Cu} and the phosphorus-on-selenium antisite P_{Se} , establish the p -type behavior and likely prevent any n -type doping near thermal equilibrium. The GGA+ U defect calculation method is shown to yield more accurate results than the more standard method of applying post-calculation GGA+ U -based bandgap corrections to strictly GGA defect calculations.

PACS numbers: 61.72.J-, 71.20.Nr, 71.15.Mb, 88.40.fh

The growing family of multinary copper chalcogenides has been of great interest for solar photovoltaic applications. In addition to the commonly used solar absorber $\text{CuIn}_{1-x}\text{Ga}_x\text{Se}_2$ (CIGS), materials that have raised interest include $\text{Cu}_2\text{ZnSnS}_4$, Cu_7TiS_4 ¹, CuClSe_2 ², CuBiS_2 ³, CuSbS_2 ³, and Cu_3BiS_3 ⁴. Recently the p -type semiconductor Cu_3PSe_4 has been established⁵ to have a direct bandgap of $E_g = 1.4$ eV, with a calculated absorption $\alpha > 5 \times 10^4 \text{ cm}^{-1}$ for wavelengths less than 630 nm. This bandgap lies in the optimal range for photovoltaic power output and warrants further investigation of the material.

In addition to optical absorption, essential considerations for photovoltaic applications include ease of synthesis, conductivity, amenability to doping, and trap-assisted charge recombination. These quantities are largely controlled by the thermodynamic stability of the material with respect to competing phases and point defects. Here we perform a point defect analysis of Cu_3PSe_4 combining the + U Hubbard term for total energy calculations with the correction methods described recently by Lany and Zunger^{6,7}. Several potential substitutional donor defects are also considered. Furthermore we examine bulk properties including the partial density of states (DOS), the dielectric tensor, and the highly asymmetric effective mass tensor. We compare our results to recent experiments⁸ and to a more standard GGA calculation. We also compare our methods with the alternative electrostatic image correction procedure described by Freysoldt *et al.*⁹.

Defect formation energies are most often calculated using density functional theory (DFT) within the local density approximation (LDA) or within the generalized gradient approximation (GGA). However, recent statistical studies^{10,11} on the accuracy of heat of formation calculations indicate that using GGA with an additional Hubbard U term for the occupation of transition metal d orbitals, the so-called GGA+ U method, will be more accurate than using standard GGA or LDA. The U value is held constant for each type of transition metal atom

throughout the analysis, including calculations of the energies of the transition metal elements themselves. These studies also suggest that one should add a statistically determined correction value to the total energy of each pure element before calculating the heat of formation ΔH of a compound. To obtain the most accurate heat of formation energies for both compounds and defects, we use GGA+ U ¹² and apply the elemental energy corrections suggested by Lany¹⁰ for P in all phosphides¹³ and for Ca in all Ca compounds. The other elements we consider, Cu, Se, Zn, Cd, and Cl, either have statistically insignificant corrections or, in the case of Cl, are not considered in Ref. [10].

Our calculations use the projector augmented wave (PAW) method^{14,15} as implemented in the plane wave code VASP¹⁶. Further details of the calculation are given in the Supplemental Material [17]. We use $U = 6$ eV for the Cu- d , Zn- d , and Cd- d orbitals. This value of U for Cu- d has been chosen in previous work (c.f. Ref. [18]) to yield agreement with the experimental band structure below the valence band maximum (VBM)¹⁹, thus eliminating the need for post-calculation corrections to the VBM of Cu_3PSe_4 .²⁰ All calculations include ionic relaxation, while lattice parameters are relaxed for all pure compounds and elements, including the defect free host.

The bonding character of Cu_3PSe_4 is evident in the GGA+ U calculation of the partial DOS, shown in Fig. 1. The valence bands above -7 eV and the conduction bands below 3.3 eV have similarities to other multinary copper chalcogenides. One such common property is that the Cu- d states are split into non-bonding e orbitals and t_2 orbitals which form filled bonding and filled antibonding bands because of their interaction with the chalcogenide p orbitals²¹. The antibonding band forms the highest valence band. Like CuInSe_2 , CuGaSe_2 , and $\text{Cu}_2\text{ZnSnSe}_4$ ²¹, the conduction band has a character that is largely antibonding between Se- p and Mt- s , where Mt represents the element acting as the high valence metal (e.g. Sn in $\text{Cu}_2\text{ZnSnSe}_4$, P in Cu_3PSe_4). The antibonding character is inferred from the presence of a spatial

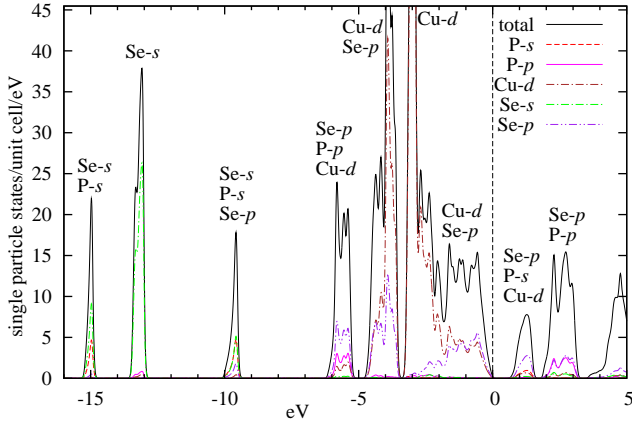


FIG. 1. (Color online) Partial density of states for the unit cell $(\text{Cu}_3\text{PSe}_4)_2$. The large Cu-d peak rises to a maximum of twice the height of the plot. The vertical dashed line at 0 denotes the valence band maximum.

TABLE I. Principal axis tensor components and appropriate scalar averages for effective hole mass (units of electron mass m_0) and electronic and total dielectric constants, ϵ_∞ and ϵ_0 . The conductivity effective mass is given by $m_{\text{cond}}^* \equiv 3/\sum_i m_i^{-1}$.

	x	y	z	scalar
m	0.10	1.66	1.82	$m^* = 0.67, \quad m_{\text{cond}}^* = 0.27$
ϵ (elect.)	14.0	13.1	12.0	$\epsilon_\infty = 13.0$
ϵ (total)	16.8	14.8	13.6	$\epsilon_0 = 15.1$

node between the Mt and Se atoms in the charge density of the lowest conduction band. Unlike materials with a metallic Mt, Cu_3PSe_4 has no valence band that is the obvious bonding counterpart. In fact, the P-s orbitals have nominally been filled in the P-s/Se-s bonding and antibonding bands, near -15 and -10 eV. This $\sigma\sigma$ bonding does not occur when Mt is more metallic, because of the larger energy difference between the atomic Mt-s level and the chalcogenide s level. Thus the appearance of a P-s/Se-p* antibond is somewhat surprising despite the fact that it follows the trend of other multinary copper chalcogenides. The bonding counterpart of the *second* conduction band, which has significant P-p/Se-p* character, is found in the valence band near -5.7 eV.

The calculated GGA+ U effective hole mass and dielectric tensor components are shown in Table I. The dielectric tensor is calculated using density functional perturbation theory²². The effective mass tensor, calculated from the band structure, has much larger components in the yz plane than along the x axis. Because the radius of a hydrogenic shallow defect state (also known as a perturbed host state⁶) is inversely proportional to effective mass, this will result in shallow acceptor wavefunctions being greatly elongated in the x direction. The defect and carrier concentration calculations below do not rely on a value of effective mass m^* , but instead use the calculated DOS directly.

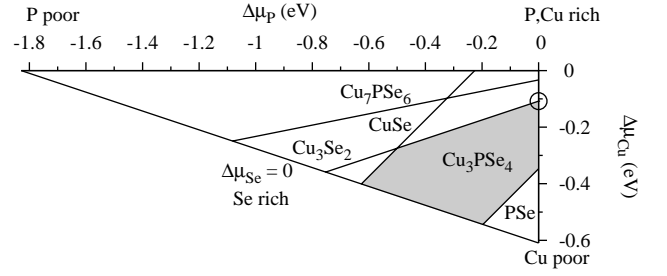


FIG. 2. Chemical potential domain with stable region of Cu_3PSe_4 in gray. The chosen Cu-rich growth condition is indicated by a circle.

We analyze the allowed chemical potential domain for Cu_3PSe_4 synthesis by calculating ΔH for 22 compounds containing Cu, P, and Se. Fig. 2 shows the results for several important compounds, revealing a relatively large stable region. To best match experimental carrier concentrations⁸, we perform the defect calculations for the conditions $\Delta\mu_{\text{P}} = 0$ and $\Delta\mu_{\text{Cu}} = -0.11$ eV (circled in Fig. 2). Choosing $\Delta\mu_{\text{Cu}}$ to assume its maximum allowed value minimizes the calculated concentration of the shallow acceptor defect V_{Cu} .

We note that it has been observed²³ that under certain conditions Cu_3PSe_4 can coexist with the ionic conductor Cu_7PSe_6 , but this is not predicted by chemical potential domain analysis. This discrepancy may be due to finite temperature effects; the low temperature α phase²⁴ of Cu_7PSe_6 was used in calculations, while at formation temperature the partially disordered γ phase would be present. We also note here that the error of total energy calculations involving phosphorus can be large; a statistical correction of 0.6 eV per P atom is given in Ref. [10] due to artifactual energy differences between phosphorus in reductive and neutral (elemental) environments. This error is expected to impart uncertainty both to the calculated heat of formation of Cu_3PSe_4 , which affects defect energies through its effect on $\Delta\mu_{\text{Cu}}$, and to the defect supercell energies themselves, particularly for the high concentration P_{Se} defect. In the latter case, the additional P atom is reduced by the neighboring Cu ions, in strong contrast to the host P atoms, which are oxidized by the Se neighbors. While phosphorus raises concern, the GGA+ U statistical corrections¹⁰ associated with Cu and Se atoms are less than 0.05 eV, and our calculated heat of formation of Cu_3Se_2 is within 0.05 eV of experiment¹⁰.

The defect analysis¹⁷ is performed initially using a $2 \times 2 \times 2$ (2^3) supercell (128 atoms). We use all finite size corrections²⁵ described by Lany and Zunger^{6,7}. No correction is made to the valence band, while the conduction band is raised so that the bandgap is increased from the calculated value of 0.52 eV to the experimental value of 1.4 eV. A shallow donor correction term⁶ $+(E_{g,\text{exp}} - E_{g,\text{calc}})$ is applied to the energies of non-ionized shallow donor defects. However, none of the in-

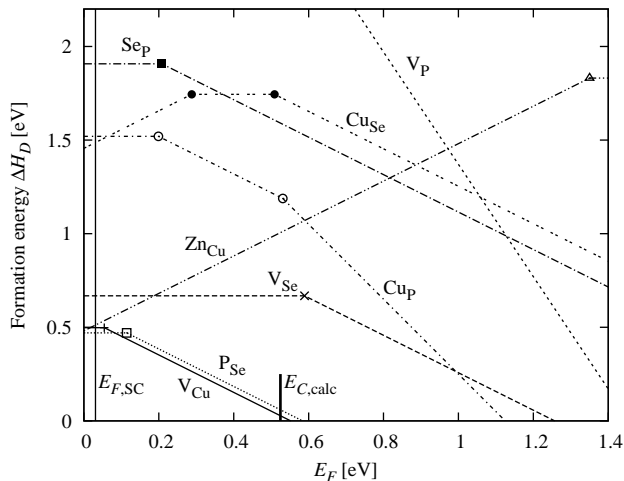


FIG. 3. Defect formation energies and transition energies. Where nonequivalent sites are calculated, the lowest energies for each charge state are shown. The self-consistent room temperature Fermi energy $E_{F,SC}$, assuming a formation temperature of 500°C, is shown by the vertical line at 0.031 eV. The (0/+) transition level for shallow donor Zn_{Cu} has been raised to follow the conduction band correction.

intrinsic point defects are clearly shallow donors, and thus this correction is applied only for the extrinsic donors considered: Ca, Cd, and Zn on a Cu site, and Cl on a Se site. As a result, none of the intrinsic defect transition energies, which are given with respect to the VBM, have been adjusted with the widening of the gap.

Formation energies and transition levels for the lower energy intrinsic defects and the lowest energy extrinsic defect are shown in Fig. 3. The acceptors V_{Cu} and P_{Se} both pin the Fermi energy below mid-gap, preventing Cu_3PSe_4 from being n -doped near thermal equilibrium. The formation energy of the neutral defect V_{Cu}^0 is calculated to be 0.50 eV, with a (-/0) transition level of 0.05 to 0.06 eV, depending on the Cu site. The formation energy of P_{Se}^0 varies with site from 0.47 eV to 0.50 eV, with the (-/0) transition levels varying from 0.08 eV to 0.17 eV.

We use the formation temperature of 500°C (approximately the temperature used in recent pellet and single crystal experiments⁸) to calculate¹⁷ the self-consistent formation temperature defect population and Fermi level. The resulting total defect concentrations (irrespective of charge state) are $4.1 \times 10^{19} \text{ cm}^{-3}$ for V_{Cu} and $4.6 \times 10^{19} \text{ cm}^{-3}$ for P_{Se} . We fix the total defect concentrations and recalculate the self-consistent populations of the various charge states at room temperature (300 K). The room temperature self-consistent Fermi level is 0.031 eV above the VBM with a hole concentration of $p = 8 \times 10^{18} \text{ cm}^{-3}$. The contribution of V_{Cu}^- to the hole density is over five times that of P_{Se}^- , indicating that V_{Cu} is electronically the most important defect type.

If zinc is present during formation, the maximum Zn_{Cu}^+ concentration is approximately $5 \times 10^{18} \text{ cm}^{-3}$, and the net room temperature hole density is lowered slightly to

TABLE II. Calculated site-averaged formation energies for V_{Cu} defects and predicted versus experimental hole concentrations. The error of the GGA+ U method is seen to be smaller than the more standard⁶ method of using GGA including VBM corrections.

	$\Delta H(V_{Cu}^0)$ [eV]	$\Delta H(V_{Cu}^-)$ [eV]	p [cm^{-3}]
GGA + VBM corr.	0.34	0.40	6×10^{19}
GGA+ U	0.50	0.56	8×10^{18}
Hall measurement ⁸	—	—	6×10^{17}

$p = 6 \times 10^{18} \text{ cm}^{-3}$. The other potential donor dopants considered have greater formation energies and can be neglected.

The V_{Cu} defect is very weakly localized and we have recalculated its two charge states on one Cu site using a 4^3 (1024 atom) supercell. Even for this supercell size, the defect wavefunction is not localized within the supercell in the x direction (the low effective mass direction). We obtain $\Delta H = 0.53$ eV for the neutral defect, with a (-/0) charge transition level of 0.04 eV. We note that the hydrogen-like approximation using the conductivity effective mass $m_{\text{cond}}^* = 0.27 m_0$ yields a comparable binding energy of 0.02 eV. Assigning the large supercell data to all Cu sites, in combination with the previous P_{Se} data, yields an insignificantly modified hole density $p = 9 \times 10^{18} \text{ cm}^{-3}$.

The P_{Se} defect state is substantially localized within the smaller 2^3 supercell and has P- p character on the defect site and Cu- d character on the nearest neighbors. The degree of localization allows us to apply the defect image charge correction of Refs. [9] using the neutral defect potential as the reference potential¹⁷. The resulting correction (0.08 eV) agrees well with the corresponding correction (image charge²⁵ + alignment²⁵ = 0.07 eV) according to Refs. [6 and 7].

The defect analysis performed here agrees qualitatively with recent experimental results. Our calculated Cu:P ratio of 2.97 is consistent with the value 2.92 ± 0.06 measured for single crystals⁸. We predict a large hole concentration of $p = 8 \times 10^{18} \text{ cm}^{-3}$, about one order of magnitude larger than the value $6 \times 10^{17} \text{ cm}^{-3}$ obtained by Hall and Seebeck measurements on pressed, sintered pellets⁸.

We compare the GGA+ U defect calculations described above with standard GGA defect calculations followed by application of a GGA+ U correction^{6,18} (-0.34 eV) to the VBM. The GGA defect calculations include all types of corrections applied to the GGA+ U calculations and include a GGA determination of the maximum allowed copper chemical potential $\Delta\mu_{Cu}$ (-0.06 eV). As shown in Table II, the more standard “GGA + VBM correction” procedure changes the formation energies of V_{Cu}^0 and V_{Cu}^- (evaluated at maximum $\Delta\mu_{Cu}$ and minimum E_F) by about -0.16 eV, causing a significantly larger overestimation of p . This comparison indicates that the superiority of GGA+ U to GGA in bulk total energy calculations^{10,11} is also extended to defect calcu-

lations.

It is instructive to consider further the implications of the available experimental results⁸. We estimate the amount by which ΔH values would have to change in order to bring the calculated hole concentration p closer to the value measured for polycrystalline pellets⁸. If one assumes that the calculated transition energy of V_{Cu} is not underestimated, the experiments of Ref. [8] indicate that the formation energy of V_{Cu} must increase, while the transition level of P_{Se} increases and the formation energy of P_{Se} decreases. The adjustment to the V_{Cu} energy must be significant to recover the measured p . For example, increasing the formation energy of V_{Cu} defects by 0.35 eV while applying changes of -0.05 and 0.05 eV to the neutral and charged P_{Se} defects respectively yields $p = 7 \times 10^{17} \text{ cm}^{-3}$ and a Cu:P ratio of 2.96. Such large changes to the V_{Cu}^q formation energies are not easily explained by calculational errors associated primarily with phosphorus.

An alternative possibility is that the GGA+ U calculated VBM is too high by a modest amount, and that the apparent shallow character of the V_{Cu} defect is an artifact of this band misplacement. For example, applying a valence band correction $\Delta E_V = -0.1$ eV and choosing not to apply the shallow acceptor corrections to the neutral defects (that is, using a strictly “band edge only” approach) yields the much lower hole concentration $p = 1.1 \times 10^{18} \text{ cm}^{-3}$ with an only slightly increased Cu:P ratio (2.976).

The experimental data suggests an increase in neutral P concentration, and possibly the presence of a low energy *donor* defect involving extra P atoms, which could lower p by compensating the V_{Cu} acceptors and thus avoid the need to raise $\Delta H(V_{Cu})$. We therefore have examined¹⁷, at lower accuracy and without finite size corrections, several configurations of neutral P interstitials I_P as well as a number of neutral two-defect complexes

of types $P_{Se}-P_{Se}$, $P_{Se}-I_P$, and I_P-I_P . The lowest complex formation energy that is less than the sum of its two parts is 1.5 eV for a $P_{Se}-I_P$ complex. The I_P formation energies range from 1.8 to 2.4 eV. Additionally, we have examined several of these defects in the +1 (active donor) charge state but have not obtained energies low enough to compete with the calculated $\Delta H(V_{Cu}^-) = 0.56$ eV. Thus no P interstitial or P-rich defect complex in the energy range of interest has been found.

In conclusion, we have performed a set of GGA+ U defect calculations on Cu_3PSe_4 , a p -type semiconductor with a direct bandgap of 1.4 eV. We compare our methods against standard GGA, larger supercells, and alternative correction methods. We predict that the V_{Cu} defect is mostly responsible for the large, experimentally observed intrinsic hole concentration p , with some contribution from P_{Se} . Both of these defects pin the Fermi level below mid-gap, so that n -doping is prohibited near thermal equilibrium. Both defects also contribute to the observed non-stoichiometric Cu:P ratio. Our calculation overestimates p by about one order of magnitude. However, the present GGA+ U method is shown to be more accurate than more standard GGA calculations with valence band corrections. Doping with Zn is calculated to have a small but noticeable effect on p . Because of the apparent uncertainty in the calculations however, this analysis does not rule out the possibility that Zn doping could significantly reduce p .

We thank Dr. Robert Kokenyesi from Oregon State University (OSU) for helpful discussions on both experimental and theoretical topics. We thank Dr. Stephan Lany from the National Renewable Energy Laboratory for very helpful discussions and for providing scripts with which some of the potential alignment and band filling corrections are calculated. This work has been supported by the National Science Foundation of the USA under Grant SOLAR DMS-1035513.

* Guenter.Schneider@physics.oregonstate.edu

¹ L. Yu and A. Zunger, Phys. Rev. Lett. **108**, 068701 (2012).

² Y. Wang, Z. Deng, X. Lv, F. Miao, S. Wan, X. Fang, Q. Zhang, and S. Yin, Mater. Lett. **63**, 236 (2009).

³ J. T. R. Dufton, A. Walsh, P. M. Panchmatia, L. M. Peter, D. Colombara, and M. S. Islam, Phys. Chem. Chem. Phys. **14**, 7229 (2012).

⁴ D. Colombara, L. Peter, K. Hutchings, K. Rogers, S. Schäfer, J. Dufton, and M. Islam, Thin Solid Films **520**, 5165 (2012).

⁵ D. H. Foster, V. Jieratum, R. Kykyneshi, D. A. Keszler, and G. Schneider, Appl. Phys. Lett. **99**, 181903 (2011).

⁶ S. Lany and A. Zunger, Phys. Rev. B **78**, 235104 (2008).

⁷ S. Lany and A. Zunger, Model. Simul. Mater. Sci. Eng. **17**, 084002 (2009).

⁸ V. Jieratum, A. J. Kokenyesi, A. J. Ritenour, L. N. Zakharov, S. W. Boettcher, J. F. Wager, and D. A. Keszler (2012) (submitted to J. Mater. Chem.).

⁹ C. Freysoldt, J. Neugebauer, and C. G. Van de Walle, physica status solidi (b) **248**, 1067 (2010); Phys. Rev. Lett. **102**, 016402 (2009).

¹⁰ S. Lany, Phys. Rev. B **78**, 245207 (2008).

¹¹ V. Stevanović, S. Lany, X. Zhang, and A. Zunger, Phys. Rev. B **85**, 115104 (2012).

¹² S. L. Dudarev, G. A. Botton, S. Y. Savrasov, C. J. Humphreys, and A. P. Sutton, Phys. Rev. B **57**, 1505 (1998).

¹³ When P is oxidized, an appropriate correction would likely have the opposite sign, and thus setting the correction to zero in these cases is a conservative measure.

¹⁴ P. E. Blöchl, Phys. Rev. B **50**, 17953 (1994).

¹⁵ G. Kresse and D. Joubert, Phys. Rev. B **59**, 1758 (1999).

¹⁶ G. Kresse and J. Furthmüller, Comput. Mater. Sci. **6**, 15 (1996).

¹⁷ See Supplemental Material at for details.

¹⁸ C. Persson, Y. Zhao, S. Lany, and A. Zunger, Phys. Rev. B **72**, 035211 (2005).

- ¹⁹ Effective U values including 4 eV²¹, 5 eV¹⁰, and 6 eV¹⁸ have been used for Cu- d to fit photoemission experiment.
- ²⁰ Such a correction would normally be made after a GGA or LDA calculation of the host material, by performing an additional calculation with the U term included and noting the change in the valence band maximum. In our case, the second calculation would be identical to the first, and thus no correction is made.
- ²¹ Y. Zhang, X. Yuan, X. Sun, B. Shih, P. Zhang, and W. Zhang, Phys. Rev. B **84**, 075127 (2011).
- ²² X. Gonze and C. Lee, Phys. Rev. B **55**, 10355 (1997).
- ²³ R. Kokenyesi (private communication).
- ²⁴ E. Gaudin, V. Petricek, F. Boucher, F. Taulelle, and M. Evain, Acta Crystallogr. Sect. B Struct. Sci. **56**, 972 (2000).
- ²⁵ The two-thirds monopole term⁶ is used for the electrostatic image corrections. The potential alignment ΔV_{PA} for both neutral and charged defects is calculated using an average of core potentials excluding the defect site, and in some cases nearest neighbor sites, as described in Ref. [7]. This alignment is applied as a correction ($+q\Delta V_{PA}$) for charged defect energies, and is also used to adjust the values of the host VBM and conduction band maximum (CBM) that are used in the band filling correction described in Ref. [6].